



Design and Optimization of Symmetric Laminated Composites using a Variable Neighbourhood Search-based Model

Jose Ignacio Pelaez, Alfonso Corz, Jose Antonio Gomez, Emilio Tenorio, Jorge Veintimilla

► To cite this version:

Jose Ignacio Pelaez, Alfonso Corz, Jose Antonio Gomez, Emilio Tenorio, Jorge Veintimilla. Design and Optimization of Symmetric Laminated Composites using a Variable Neighbourhood Search-based Model. Engineering Optimization, 2011, pp.1. 10.1080/0305215X.2011.588225 . hal-00734186

HAL Id: hal-00734186

<https://hal.science/hal-00734186>

Submitted on 21 Sep 2012

HAL is a multi-disciplinary open access archive for the deposit and dissemination of scientific research documents, whether they are published or not. The documents may come from teaching and research institutions in France or abroad, or from public or private research centers.

L'archive ouverte pluridisciplinaire **HAL**, est destinée au dépôt et à la diffusion de documents scientifiques de niveau recherche, publiés ou non, émanant des établissements d'enseignement et de recherche français ou étrangers, des laboratoires publics ou privés.



Design and Optimization of Symmetric Laminated Composites using a Variable Neighbourhood Search-based Model

Journal:	<i>Engineering Optimization</i>
Manuscript ID:	GENO-2011-0005.R2
Manuscript Type:	Original Article
Date Submitted by the Author:	29-Apr-2011
Complete List of Authors:	Pelaez, Jose; University of Malaga, Dep.Languages and Computer Sciences corz, alfonso; Cadiz University, Civil and Industrial Engineering Gomez, Jose; Malaga University, Languages and Computer Sciences tenorio, Emilio; Malaga University, Languages and Computer Sciences Veintimilla, Jorge; Malaga University, Engineering, Materials and Production
Keywords:	VNS, composite materials, soft computing, materials desing

SCHOLARONE™
Manuscripts

**Design and Optimization of Symmetric Laminated Composites using
a Variable Neighbourhood Search-based Model**

Corz A.[†] Gómez-Ruiz J.A.^{††} Peláez J.I.^{††*} Tenorio E.^{††} Veintimilla J.^{†††}

[†]*Department of Civil and Industrial Engineering*

Cadiz University, Algeciras, Spain

^{††}*Department of Languages and Computer Sciences*

Malaga University, Malaga 29071, Spain

*Corresponding author. Email: jignacio@lcc.uma.es

^{†††}*Department of Civil Engineering, Materials and Production*

Malaga University, Malaga 29071, Spain

Design and Optimization of Symmetric Laminated Composites using a Variable Neighbourhood Search-based Model

The development of society is still marked by the need for lighter and stronger structures. The materials that respond best to these needs are composite materials. Designing composite materials is difficult as it involves designing the geometry and their composition. Traditionally, the design tasks have been based on approximate methods; the possibility for creating composite materials is almost unlimited, characterization by testing is very expensive and it is difficult to apply the results to other contexts. This article proposes a Variable Neighbourhood Search-based Model for the design of Symmetric Laminated Composites, a general encoding for the design of composites, an evaluation function that has taken into consideration cost and safety criteria in design, the neighbourhood structures and a set of local search operators. The proposed model has been applied to different real-world problems and the results have been compared with other well-known design methods.

Keywords: VNS, Soft Computing, Composite Materials, Materials Design

1. Introduction

A composite material, or composite, is made by combining two or more materials to form another one that is appropriate for a specific application. The agglomerate material is known as the matrix, and the remaining are the reinforcement materials that may be made up of continuous fibres, short fibres or particles (Barbero, E.J., 1999; Gürdal, Z. *et al.* 1999). When the design is sufficient, the new material adopts the best properties of their constituents, and sometimes even some that none of these possess. The properties that the design of a composite material aims to improve on are strength, stiffness, toughness, lightness, thermal insulation, etc. Of course, not all of them can be improved simultaneously so the design objective is to obtain a new material that offers the best possible adaptation to the required specifications.

Figure 1 shows an assessment of different composite materials and metals based on the properties of strength and specific stiffness. For example, a unidirectional lamina based on continuous Kevlar 49 fibres, has a much higher specific strength than steel or aluminium and yet has comparable stiffness. In the case of unidirectional laminas based on continuous graphite fibres, similar strength and greater stiffness is achieved.

Although composite materials, such as the addition of straw to mud or the use of laminated wood, have been used since ancient times, the real boom has only happened recently with the development of materials based on a fibre reinforced resin matrix (Duratti, L. *et al.* 2002). The exceptional strength and lightness of these materials has led to the development of an enormous number of applications, particularly in the aeronautical and space industries due to the economic significance of these properties.

However, this type of material is difficult to develop, because the design of a new composite material involves designing both, the geometry of the element and the configuration of the material itself so as to best exploit the qualities of the constituent materials. The deterioration of the properties over time due to stress, which can lead to unanticipated behaviour (breaks) or failure of the structural element in question, must also be evaluated (Puck, A. & Schurmann, H., 1998 & 2002).

The composites with unidirectional reinforcement of the fibres made up of laminas of the same composition, stacked and bound together by the same material that forms the matrix, but with distinct fibre orientation, are particularly important. From now on, this type of element will be referred to as laminate. Within this category, symmetric laminates are worthy of special attention, with both geometrical and structural symmetry relative to their mean surface. Figure 2 depicts the composition of a lamina as well as the laminate construction.

To manufacture laminates, laminas are stacked in such a way that the strength and stiffness of the material depends on the number and orientation of these laminas (Gürdal, Z. *et al.* 1999). The degree of compatibility of the reinforcement, the production method and the geometry of the element must all be tested and a suitable manufacturing process must be found in order to ensure the quality of the finished product (Car, E. *et al.* 2000; Stellbrink, K.U., 1996).

The design process for a laminate starts with the definition of the problem to be solved and the specifications to be met by the element to be designed. From this information, a series of solutions are generated by a synthesis process that is usually, primarily, supported by the expertise of the designer. Potentially viable solutions are subsequently analysed to test their effectiveness. This analysis of viable solutions is made using a finite element modelling based software package, *i.e.* ANSYS®, that is used usually in industry. This whole process is an iterative task that allows the proposed solution to be repeatedly improved until the final design is obtained. Traditionally, the design work, both synthesis and analysis has been carried out using empirical knowledge based methods (Grosset, L. *et al.* 2006). This is partly because the number of possible combinations of composites is almost unlimited and also because characterization by experimentation is very expensive.

Since 1990 different design systems have been proposed which aim to overcome these limitations. These proposals have involved approaches ranging from traditional techniques such as classical nonlinear optimization procedures combined with finite element modelling (FEM) (Huang, J. & Haftka, R.T., 2005; Matthews, F.L. *et al.* 1999), through generic task methods and case-based reasoning (Lenz, T.J., 1997), to modern artificial intelligence techniques (Adams D.B. *et al.* 2003; Falkenauer, E., 1998; Soremekun, G. *et al.* 2001 & 2002; McMahon M.T., & Watson L.T., 2000).

At present, one technique that proves more efficient in a large number of situations is the Variable Neighbourhoods Search (VNS) method (Hansen, P. *et al.* 2003). This metaheuristic, proposed in 1995 by Mladenovic (Mladenovic, N., 1995), is based on a systematic change of neighbourhood, with local search, that aims to improve the value of the target function in each neighbourhood. Figure 3 outlines the basis structure of this metaheuristic (Mladenovic, N. & Hansen, P., 1997).

Figure 4 shows how VNS metaheuristic works when looking for a function minimum.

The article is organized as follows: section 2 relates to the analysis of symmetric laminates; section 3 presents a model for the designing and optimization of symmetric laminates based on the VNS metaheuristic; in section 4, this model is applied to several real applications and the results are compared with other methods to prove its worth; and finally, conclusions are presented in section 5.

2. Analysis of Symmetric Laminates

Composite laminates are considered as orthotropic materials, with different properties in three mutually perpendicular directions at a point. Because of their low thickness sizes, they can be modelled as shells. In this section we consider the mechanical analysis of a symmetric laminate to determine the numbers of laminae that break, a factor that is used in the definition of the fitness function.

2.1. Strain-Stress Relations in an Orthotropic Lamina

A unidirectional reinforced lamina is made up of a set of very thin fibres, aligned in a particular direction, and embedded in a polymeric matrix that supports them. The relative amounts of the two components are expressed as the fibre and matrix volume

fraction, V_f and V_m , which are dimensionless quantities and must satisfy that $V_f + V_m = 1$. V_f is usually between 0,3 and 0,7. For a lamina in the 1-2 plane, a plane stress state is defined by setting

$$\sigma_3 = 0; \quad \tau_{23} = 0; \quad \tau_{31} = 0 \quad (1)$$

The characteristics of a lamina are defined by their elastic constants: Young's modulus for the principal directions, E_1 and E_2 ; stiffness modulus, G_{12} ; and Poisson ratio, ν_{12} . These constants are in turn dependent on the properties of the fibre and the matrix: Young's modulus, E_f and E_m ; Poisson coefficients, ν_f and ν_m ; as well as the shape and size of the fibres, their distribution and volume fraction, V_f , etc.

Using Equation (1), strain-stress relations can be formulated as

$$\begin{pmatrix} \varepsilon_1 \\ \varepsilon_2 \\ \gamma_{12} \end{pmatrix} = \begin{pmatrix} S_{11} & S_{12} & 0 \\ S_{12} & S_{22} & 0 \\ 0 & 0 & S_{66} \end{pmatrix} \cdot \begin{pmatrix} \sigma_1 \\ \sigma_2 \\ \tau_{12} \end{pmatrix} \quad (2)$$

where

$$S_{11} = \frac{1}{E_1}; \quad S_{22} = \frac{1}{E_2}; \quad S_{12} = -\frac{\nu_{12}}{E_1} = -\frac{\nu_{21}}{E_2}; \quad S_{66} = \frac{1}{G_{12}} \quad (3)$$

2.2. Strain-Stress Relations for a Lamina of Arbitrary Orientation

In case that the principal material axes, 1-2, do not coincide with the natural axes for the solution of the problem, X-Y, the lamina stops behaving orthotropically and all the

elements of the stiffness matrix take non-zero values. Figure 5 sets out the labelling system used from now on for the orientation of the laminas.

In this case, the stress relation is

$$\begin{pmatrix} \sigma_x \\ \sigma_y \\ \tau_{xy} \end{pmatrix} = [T]^{-1} \cdot \begin{pmatrix} \sigma_1 \\ \sigma_2 \\ \tau_{12} \end{pmatrix} \quad (4)$$

where $[T]$ is the coordinate transformation matrix

$$[T] = \begin{pmatrix} \cos^2 \theta & \sin^2 \theta & 2 \cdot \sin \theta \cdot \cos \theta \\ \sin^2 \theta & \cos^2 \theta & -2 \cdot \sin \theta \cdot \cos \theta \\ -\sin \theta \cdot \cos \theta & \sin \theta \cdot \cos \theta & \cos^2 \theta - \sin^2 \theta \end{pmatrix} \quad (5)$$

Similarly, the strain relation is obtained and, after several operations, it leads to the following stress-strain relation

$$\begin{pmatrix} \sigma_x \\ \sigma_y \\ \tau_{xy} \end{pmatrix} = [\bar{Q}] \cdot \begin{pmatrix} \epsilon_x \\ \epsilon_y \\ \gamma_{xy} \end{pmatrix} \quad (6)$$

where $[\bar{Q}]$ is the transformed stiffness matrix [2].

2.3. Loads and Moments of Symmetric Laminates

A symmetric laminate has its mid-plane as a plane of symmetry, so that any lamina at a given distance above the mid-plane has an identical lamina at the same distance below

the mid-plane. Using integration over thickness of a lamina, loads and moments can be obtained as

$$\begin{Bmatrix} \mathbf{N} \\ \mathbf{M} \end{Bmatrix} = \begin{bmatrix} \mathbf{A} & \mathbf{B} \\ \mathbf{B} & \mathbf{D} \end{bmatrix} \cdot \begin{Bmatrix} \boldsymbol{\varepsilon}^0 \\ \boldsymbol{\kappa} \end{Bmatrix} \quad (7)$$

where $\mathbf{N} = \{N_x, N_y, N_{xy}\}$ and $\mathbf{M} = \{M_x, M_y, M_{xy}\}$ are loads and moments vectors; $\boldsymbol{\varepsilon}^0$ and $\boldsymbol{\kappa}$ are strain and curvature of middle plane; \mathbf{A} is extensional stiffness matrix, \mathbf{B} is coupling stiffness matrix ($\mathbf{B} = \mathbf{0}$ for a symmetric laminate) and \mathbf{D} is bending stiffness matrix [2].

2.4. Lamina Breakage Coefficients (P_k^I)

Different failure criteria are used to determine whether a lamina can withstand specific stress conditions without breaking (Barbero, E.J., 1999). In this article we have selected the Tsai-Wu tensor failure criterion (Tsai, S.W & Wu, E.M., 1971), that postulates that a failure surface in six-dimensional stress space exists in the form

$$F_i \cdot \sigma_i + F_{ij} \cdot \sigma_{ij} = 1 \quad i, j = 1, \dots, 6 \quad (8)$$

wherein F_i and F_{ij} are strength tensors of the second and fourth rank, respectively, and the usual contracted stress notation is used ($\sigma_4 = \tau_{23}$, $\sigma_5 = \tau_{31}$ and $\sigma_6 = \tau_{12}$). In the case of an orthotropic lamina under plane stress conditions, we have the relation

$$\left(\frac{1}{\bar{X}} - \frac{1}{\bar{X}'}\right) \cdot \sigma_1 + \left(\frac{1}{\bar{Y}} - \frac{1}{\bar{Y}'}\right) \cdot \sigma_2 + \frac{1}{\bar{X} \cdot \bar{X}'} \cdot \sigma_1^2 + \frac{1}{\bar{Y} \cdot \bar{Y}'} \cdot \sigma_2^2 - \sqrt{\frac{1}{\bar{X} \cdot \bar{X}' \cdot \bar{Y} \cdot \bar{Y}'}} \cdot \sigma_1 \cdot \sigma_2 + \frac{1}{\bar{S}^2} \cdot \tau_{12}^2 = 1 \quad (9)$$

where X, X', Y, Y' and S are, respectively, the ultimate tensile and compressive strength in the fibre direction, the ultimate tensile and compressive transversal strength, and the shear strength. In order to determine if a lamina breaks, we establish a breakage coefficient P_k , defined as:

$$P_k = \left(\frac{1}{X} - \frac{1}{X'}\right) \cdot \sigma_1 + \left(\frac{1}{Y} - \frac{1}{Y'}\right) \cdot \sigma_2 + \frac{1}{X \cdot X'} \cdot \sigma_1^2 + \frac{1}{Y \cdot Y'} \cdot \sigma_2^2 - \sqrt{\frac{1}{X \cdot X' \cdot Y \cdot Y'}} \cdot \sigma_1 \cdot \sigma_2 + \frac{1}{S^2} \cdot \tau_{12}^2 \quad (10)$$

For each lamina 'i' of a laminate, its breakage coefficient P_k^i will be used in the next section to determine the fitness function. The laminate does not break if $P_k^i \leq 1, \forall i$, and breaks otherwise. Besides, if $P_k^i \cong 1$, the lamina 'i' is working at full capacity.

3. A VNS-based Model for the Designing of Symmetric Laminates

This section presents a model based on VNS for the designing of symmetric laminates. The optimization problem, an encoding scheme for the representation of the problem, a fitness function to evaluate the feasibility of solutions, the neighbourhood structures and a set of local search operators are presented.

3.1. Optimization Problem

The optimization problem can be formulated as finding the material (fiber F and matrix M), the volume fraction VF and the orientation of the laminas of the laminate $\theta_1, \dots, \theta_m$ in order to minimize the number of laminas n . The set of design variables is expressed as a vector $\mathbf{s} = (F, M, VF, \theta_1, \dots, \theta_m)$. The optimization problem with appropriate constraints can be expressed as

$$\min_{\mathbf{s}} f(\mathbf{s}) \quad (11)$$

such that

$$\begin{aligned} n &\geq 2 && \text{(number of laminas)} \\ R_k^i &\leq 1, \forall i && \text{(Tsai - Wu coefficients)} \\ VF &\in [0.3, 0.7] \text{ in } 0.1 \text{ intervals} && \text{(volume fraction)} \\ \theta_i &\in [-80^\circ, 90^\circ], \text{ in } 10^\circ \text{ intervals} && \text{(orientation of the laminas)} \end{aligned} \quad (12)$$

3.2. Encoding

The structure of the laminate will be represented by a set of four elements (see Fig. 6). These elements are the fiber, the matrix, the volume fraction and the laminate geometry. Fitness shows how well adapted the solution is to its environment, and is added to the structure.

Each of the four elements that define the laminate represents a different characteristic of its composition: Fiber and Matrix are represented by an integer number; Volume Fraction, by a real number; and Geometry by a sequence of integers that represents the direction of fibers.

To represent the geometry of the laminate, we use the following criteria: [70 -40 0 10 -60 20] is a symmetric laminate whose outer (first) lamina has an orientation of 70°, the second one (next) of -40°, and so on.

3.3. Fitness

The fitness function takes into account economic and safety criteria. For this reason, whilst alignment of stresses along the direction of the fibres is favoured in the numerator, the denominator penalizes the following: stacking more than four consecutive laminas with the same fibre orientation; volume fraction and high laminate thickness; lamina breakage; and the distribution of stress in directions other than that of the fibres. The higher the value of fitness function, the better the solution.

The fitness function, F , is defined as follows:

$$F = 10^{\alpha} \cdot \frac{P_1^{\beta}}{(CLA + 1) \cdot VF \cdot (n \cdot e)^{\gamma} \cdot (R + 1)^{\delta} \cdot (P_2 + 1) \cdot (P_{12} + 1)} \quad (13)$$

where the coefficients are described in Table 1.

The objective of the factor 10^{α} is to maintain the Fitness between manageable values. The exponent α has been empirically determined as -28.

3.4. Neighbourhood Structures

The neighbourhood structures are a set of functions that associate a set of local solutions, called a neighbourhood, with each solution. Given the characteristics of the problem, two neighbourhood structures are proposed and defined as NS_1 and NS_2 (see Table 2).

3.5. Local Search Operators

The operators proposed in the model are summarized in Table 3.

4. Experimental Results

The model proposed in this article is applied to three designing problems. These problems have been chosen because, with minor variations, they cover a wide range of real problems.

The results obtained are compared with three other heuristics in order to verify the advantages. These heuristics are a Simulated Annealing, a Tabu Search and a Standard Genetic algorithm, that use the same representation of the problem proposed in this work. In simulations the values for the encoding are shown in Table 4.

4.1. Thin-Walled Ring under Internal Pressure

The problem is to determine the composition and thickness, t , of a circular ring, where t is small compared to the average radius, r , and subjected to internal pressure, p . Figure 7 illustrates the circular ring along with the stresses on an element of it.

The force resulting from the equilibrium equation is defined as:

$$N_x = p \cdot r$$

For example, if $p = 50 \text{ Kg/cm}^2 = 4.9050 \text{ MPa}$ and $r = 1 \text{ m}$

$$N_x = p \cdot r = 4.9050 \cdot 10^6 \cdot 1 = 4.9050 \cdot 10^6 \text{ N/m}$$

Table 5 presents the statistics corresponding to 300 tests completed with all heuristics. The results obtained with the VNS-based model are compared to the other heuristics. For each model, the results shown correspond to the least number of laminas of the material obtained, $N_{L_{min}}$, the number of times this solution is obtained N_l , its average \overline{NL} , and its standard deviation σ_{NL} . Also the best (maximum) fitness obtained, F_{max} , and its average \overline{F} are presented.

Comparing the results obtained in Table 5, it can be denoted that the VNS-based model offers better results because there is very little deviation in the solutions obtained and a much higher value for the fitness function. Moreover the proposed model obtains a material with the lowest number of layers.

Figure 8 shows the histograms corresponding to the number of laminas and the fitness of laminates obtained by the VNS-based model.

In Table 6, the specifications of the best laminate obtained with the VNS-based model and the best laminates obtained with the other techniques are shown. The angles are measured relative to the circumferential direction.

All the solutions obtained by VNS-based model have been validated by the ANSYS® software package offering values of $P_k^i \leq 1$, that is, the laminas do not break. Also, in Table 7, the P_k^i coefficients obtained in the best solution of VNS-based model are shown.

This example does not achieve much uniformity of the coefficients P_k^i around 1; this is the penalty paid for not letting more than four contiguous layers with the same orientation, due to the apparition of thermal stresses during the curing process (Gürdal, Z. *et al.* 1999). With this restriction, the laminas with 10° and -10° orientations get the failure state in first place, resulting in that the laminas with an angle of 0° do not work near its full capacity.

In case of not considering such a constraint, the results, only for the VNS case, are represented in Tables 8 to 10:

In this case, all the laminas almost reach the value 1 for P_k^i coefficients, and its number has reduced considerably.

4.2. Thin-Walled Circular Tank under Internal Pressure

The problem is to determine the composition and thickness, e , of a cylindrical tank, where e is small compared to the average radius, r , and subjected to internal pressure p . Figure 9 shows the cylindrical tank along with the stresses on an element of it.

The forces resulting from the equilibrium equation are defined as:

$$N_x = p \cdot r \quad N_y = \frac{p \cdot r}{2}$$

For example, if $p = 18 \text{ Kg/cm}^2 = 1.7685 \text{ MPa}$ and $r = 1 \text{ m}$

$$N_x = p \cdot r = 1.7685 \cdot 10^6 \cdot 1 = 1.7685 \cdot 10^6 \text{ N/m}$$

$$N_y = \frac{p \cdot r}{2} = \frac{1.7685 \cdot 10^6 \cdot 1}{2} = 0.8829 \cdot 10^6 \text{ N/m}$$

Table 11 shows the statistics corresponding to 300 tests completed with all heuristics. It can be denoted that the VNS-based model obtains the best results.

Figure 10 shows the histograms corresponding to the number of laminas and the fitness of laminates obtained by the VNS-based.

In Table 12, the specifications of the best laminate obtained with the VNS-based model and the best laminates obtained with the other techniques are shown. The angles are measured relative to the circumferential direction.

Also in this problem, all solutions obtained by VNS-based model have been validated by the ANSYS[®] software package offering values of $P_k^i \leq 1$, that is, the laminas do not break. In Table 13, the P_k^i coefficients obtained in the best solution of VNS-based model are shown.

4.3. Hollow Driveshaft under Torsion

The problem is to determine the composition and thickness, e , of a driveshaft, where e is small compared to the average radius, r , and subjected to an external torque T . Figure 11 shows the driveshaft along with the stresses on an element of it.

The force resulting from the equilibrium equation are defined as:

$$N_{xy} = \frac{T}{2 \cdot \pi \cdot r^2}$$

For example, if $T = 40000 \text{ N} \cdot \text{m}$ and $r = 0.05 \text{ m}$

$$N_{xy} = \frac{T}{2 \cdot \pi \cdot r^2} = \frac{40000}{2 \cdot \pi \cdot 0.05^2} = 2.54648 \cdot 10^6 \text{ N/m}$$

Table 14 shows the statistics corresponding to 300 tests completed with all heuristics. Again, it can be denoted that the VNS-based model obtains the best results.

Figure 12 shows the histograms corresponding to the number of laminas and the fitness of laminates obtained by the VNS-based.

In Table 15, the specifications of the best laminate obtained by the VNS-based model and the best laminates obtained with the other techniques are shown. The angles are measured relative to the circumferential direction.

Also in this problem, all solutions obtained by VNS-based model have been validated by the ANSYS® software package offering values of $P_H^i \leq 1$, that is, the laminas do not break. In Table 16, the P_H^i coefficients obtained in the best solution of VNS-based model are shown.

5. Conclusions

In this article the design of the geometry and composition of symmetric laminated composite materials is studied. In particular we have proposed a Variable Neighbourhood Search-based Model for the design of Symmetric Laminated Composites.

This model proposes a general encoding for the design of composites, a fitness function that takes into account economic and safety criteria in design, the neighbourhood structures and a set of local search operators. These local search

operators allow a lamina to be added or removed, to change its orientation, to change the type of matrix or fibre, to change volume fraction, and some others.

The VNS-based proposed model has been applied to different real-world problems and the results have been compared with other well-known design methods. The F_k (Tsai-Wu) coefficients obtained are closest to 1 in all laminas, meaning that all laminas of the composite material work near to their strength limits with consequent more efficient use of the material.

All solutions obtained by the VNS-based proposed model have been validated by the ANSYS[®] software package.

References

Adams D.B. *et al.* 2003. Optimization and blending of composite laminates using genetic algorithms with migration. *Mechanics of Advanced Materials and Structures*, 10 (3), 183-203.

Ansys Inc., 2007. Ansys Release 11.0.

Barbero, E.J., 1999. *Introduction to composite materials design*. Philadelphia, Pa.; Taylor & Francis.

Car, E. *et al.* 2000. *Tratamiento numérico de los materiales compuestos*. Barcelona: Centro Internacional de Métodos Numéricos en Ingeniería.

Duratti, L. *et al.* 2002. Selecting the components of polymeric composites. *Advanced Engineering Materials*, 4 (6), 367-371.

Falkenauer, E., 1998. *Genetic Algorithms and Grouping Problems*. New York: John Wiley and Sons.

Grosset, L. *et al.* 2006. A double-distribution statistical algorithm for composite laminate optimization. *Structural and Multidisciplinary Optimization*, 31 (1), 49-59.

Gürdal, Z. *et al.* 1999. *Design and optimization of laminated composite materials*. New York: John Wiley and Sons.

Hansen, P. *et al.* 2003. Variable Neighbourhood Search. *Inteligencia Artificial, Revista Iberoamericana de Inteligencia Artificial*, 19, 77-92.

Huang, J. & Haftka, R.T., 2005. Optimization of fibre orientations near a hole for increased load carrying capacity of composite laminates. *Structural and Multidisciplinary Optimization*, 30 (5), 335-341.

Lenz, T.J., 1997. *Designing composite material systems using generic tasks and case-based reasoning*. Thesis (PhD). Michigan State University.

Matthews, F.L. *et al.* 1999. *Finite element modelling of composite materials and structures*. UK: Imperial College, University of London.

McMahon M.T., & Watson L.T., 2000. A distributed genetic algorithm with migration for the design of composite laminate structures. *International Journal of Parallel, Emergent and Distributed Systems*, 14 (4), 329-62.

Mladenovic, N., 1995. A Variable Neighborhood Algorithm: A New Metaheuristics for Combinatorial Optimization. In *Abstract for articles presented at Optimization Days*, page 112, Montreal, Canada.

Mladenovic, N. & Hansen, P., 1997. Variable Neighborhood Search. *Computers and Operations Research*, 24 (11), 1097-1100.

Puck, A. & Schurmann, H., 1998. Failure analysis of FRP laminates by means of physically based phenomenological models. *Composite Science and Technology*, 58 (7), 1045-1067.

Puck, A. & Schurmann, H., 2002. Failure analysis of FRP laminates by means of physically based phenomenological models. *Composite Science and Technology*, 62 (12-13), 1633-1672.

Soremekun, G. *et al.* 2001. Composite laminate design optimization by genetic algorithm with generalized elitist selection. *Computers & Structures*, 79 (2), 131-143.

Soremekun, G. *et al.* 2002. Stacking sequence blending of multiple composite laminates using genetic algorithms. *Composite Structures*, 56 (1), 53-62.

Stellbrink, K.U., 1996. *Micromechanics of Composites: Composite Properties of Fibre and Matrix Constituents*. Munich: Hanser.

Tsai, S.W & Wu, E.M., 1971. A General Theory of Strength for Anisotropic Materials. *Journal of Composite Materials*, 5 (1), 58-80.

Table 1. Fitness equation coefficients

Coeff.	Description
P_1	Longitudinal coefficient along the direction of the fibres. It is a real value indicating the relationship between longitudinal stress in the direction of the fibres and the breakage stress in that direction. As the direction of the fibres is that of most resistance, it is of interest that this ratio be as high as possible. For this reason, it is in the numerator. The exponent β has been empirically determined as 2. $P_1 = \sum_i \left(\left \frac{\sigma_1^i}{X^i} \right ^\beta \right) v_i \left \frac{\sigma_1^i}{X^i} \right $ where the stress σ_1^i is either tensile or compressive and the sum applies to the laminas that do not break
P_2	Longitudinal coefficient perpendicular to the direction of the fibres. It is a real value that indicates the relationship between the longitudinal stress perpendicular to the fibres and the breakage stress in that direction. As the direction perpendicular to the fibres is that of least resistance, it is of interest that this ratio be as small as possible. For this reason it is in the denominator. $P_2 = \sum_i \left(\left \frac{\sigma_2^i}{Y^i} \right ^\beta \right) v_i \left \frac{\sigma_2^i}{Y^i} \right $ where the stress σ_2^i is either tensile or compressive and the sum applies to all the laminas
P_{12}	Shear coefficient. It is a real value that indicates the relationship between the shear stress in the plane and the maximum stress that can be tolerated in that plane. As the lamina has low resistance to these stresses,

	it is of interest that this ratio is as small as possible. For this reason it is in the denominator. The sum applies to all the laminas. $R_2 = \sum_i \left \frac{r_{12}^i}{s^i} \right $
CLA	Coefficient that indicates whether the number of adjacent layers with the same orientation is less than or equal to four (CLA = 0) or greater than four (CLA = 10^{10}). It is in the denominator so as to heavily penalise this second possibility. Its values have been empirically determined.
VF	Fiber volume fraction of the laminate. As this value should tend towards small values that are more advantageous economically, it is placed in the denominator where small values will have a positive effect.
$n \cdot e$	Product of the number of laminas and its thickness (lamina thickness is expressed in meters, but to keep the Fitness dimensionless, it is divided by 1 meter). This value must be as small as possible, so it is in the denominator. The exponent γ has been empirically determined as 12.
R	Indicates the number of layers that break ($P_{ik}^i > 1$), and is in the denominator in order to penalize such an event. The exponent δ has been empirically determined as 4.

Table 2. Neighbourhood structures

Neighbourhood structure	Description
NS₁	The set of solutions generated, keeping constant the number of layers in the original solution, and varying the other characteristics (orientation of the laminas, fiber, matrix, volume fraction)
NS₂	The set of solutions whose number of laminas is comprised in a certain range, which depends on whether the original solution breaks or not. If the laminate breaks, the neighbourhood includes all solutions whose number of laminas is in the range $n_0 - \alpha \leq n \leq n_0 + \alpha$, where n_0 is the number of laminas in the original solution. If the laminate does not break, the range is $n_0 - \beta \leq n \leq n_0$. In both cases, the remaining characteristics are also variable. Empirically, we have determined that the best values for α and β are 3 and 6, respectively.

Table 3. Local search operators

Operator	Description
BringNear_0	Operates on the geometry gene of the laminate, varying the orientation of the laminas, moving each one of them 10° closer to 0°. If the orientation of any one lamina is 0°, it is left unchanged. The objective of this operator is to obtain individuals that better withstand longitudinal stress along the X axis. $[50 \ -30 \ 0 \ 10 \ -70 \ 30]_s \rightarrow [40 \ -20 \ 0 \ 0 \ -60 \ 20]_s$
BringNear_90	Operates on the geometry gene of the laminate, varying the orientation of the laminas, moving each one of them 10° closer to 90°. If the orientation of any one lamina is 90°, it is left unchanged, and if it is -80° it is changed to 90°. The objective of this operator is to obtain individuals that better withstand longitudinal stress along the Y axis. $[20 \ 60 \ -80 \ -10 \ 30 \ -50]_s \rightarrow [30 \ 70 \ 90 \ -20 \ 40 \ -60]_s$
BringNear_45	Operates on the geometry gene of the laminate, varying the orientation of the laminas, moving each one of them 10° closer to +45° or -45°, depending on whether it is positive or negative. If the orientation of any one lamina is 40°, 50°, -40° or -50°, it is left unchanged, and if it is 0° it is changed to 10°. The objective of this operator is to obtain individuals that better withstand shear stress. $[-30 \ 40 \ -50 \ -10 \ 90 \ 20 \ -40]_s \rightarrow [-40 \ 40 \ -50 \ -20 \ 80 \ 30 \ -40]_s$
Add_1_Lamina	Operates on the geometry gene of the laminate, adding an individual lamina with random orientation and positioning. If the number of laminas is already the maximum possible, it is left unchanged. The objective of this operator is to explore in the direction of the greatest number of laminas. $[30 \ 70 \ 90 \ -20 \ 40 \ -60]_s \rightarrow [30 \ 70 \ -10 \ 90 \ -20 \ 40 \ -60]_s$
Remove_1_Lamina	Operates on the geometry gene of the laminate, removing an individual lamina, chosen at random. If there is only one lamina, it is left unchanged. The objective of this operator is to explore in the direction of the least number of laminas. $[-20 \ 70 \ 90 \ -30 \ -50 \ 20 \ -40]_s \rightarrow [-20 \ 70 \ 90 \ -50 \ 20 \ -40]_s$

Change_Orientation	Operates on the geometry gene of the laminate, changing the orientation of a lamina, chosen at random and relocated in a new position, also chosen at random. The objective of this operator is to explore in the direction of new orientations. [50 60 -10 -60 30 -20] _s → [50 -20 -10 -60 30 -20] _s
Change_Fibre	Operates on the fibre gene, changing it for a distinct one, chosen at random. The objective of this operator is to explore in the sub-space of the fibres, maintaining constant the matrix, the volume fraction, the number of laminas and their orientation. [P-100] → [Boron]
Change_Matrix	Operates on the matrix gene, changing it for a distinct one, chosen at random. The objective of this operator is to explore in the sub-space of the matrices, maintaining constant the fibre, the volume fraction, the number of laminas and their orientation. [Peek] → [Polyamide]
Change_F_Vol	Operates on the volume fraction gene of the individual, changing its value for a distinct one, chosen at random, within the acceptable limits. The objective of this operator is to explore in the sub-space of the volume fractions, maintaining constant the fibre, the matrix, the number of laminas and their orientation. [0.5] → [0.7]

Table 4. Encoding used for simulations

Elements	Values												
Fiber	A set of eleven fibres are used, each represented by an integer number.												
	<table><tr><td>1</td><td>2</td><td>3</td><td>4</td><td>5</td><td>6</td></tr><tr><td>E-Glass</td><td>S-Glass</td><td>AS-1</td><td>AS-4</td><td>IM-7</td><td>P-100</td></tr></table>	1	2	3	4	5	6	E-Glass	S-Glass	AS-1	AS-4	IM-7	P-100
	1	2	3	4	5	6							
	E-Glass	S-Glass	AS-1	AS-4	IM-7	P-100							
	<table><tr><td>7</td><td>8</td><td>9</td><td>10</td><td>11</td></tr><tr><td>T-40</td><td>T-300</td><td>Boron</td><td>Kevlar-49</td><td>Kevlar-149</td></tr></table>	7	8	9	10	11	T-40	T-300	Boron	Kevlar-49	Kevlar-149		
7	8	9	10	11									
T-40	T-300	Boron	Kevlar-49	Kevlar-149									
Matrix	A set of five matrices are used, each represented by an integer number.												
	<table><tr><td>1</td><td>2</td><td>3</td><td>4</td><td>5</td></tr><tr><td>Peek</td><td>PPS</td><td>Polyester</td><td>Epoxy</td><td>Polyamide</td></tr></table>	1	2	3	4	5	Peek	PPS	Polyester	Epoxy	Polyamide		
	1	2	3	4	5								
Peek	PPS	Polyester	Epoxy	Polyamide									
Volume fraction	A real number from the set {0.3, 0.4, 0.5, 0.6, 0.7} [1]												
Geometry of the laminate	A sequence of integers, one for each lamina, in the range [-80°, +90°], in 10° intervals												

Table 5. Statistics corresponding to the series of tests

Algorithm	$NL_{feasible}$	N_I	\overline{NL}	σ_{NL}	F_{max}	\overline{F}
VNS-based model	14	124	15.5933	1.7716	20334.20	9187.60
Genetic Algorithm	34	1	68.4933	10.9323	3.9470	0.317
Simulated Annealing	*	*	*	*	*	*
Tabu Search	*	*	*	*	*	*

* This algorithm is unable to find a feasible solution

Table 6. Characteristics of the best laminate obtained in a series of tests

Algorithm	Fibre	Matrix	VF	Fitness	Laminas	Thickness (mm)
VNS-based model	IM-7	Peek	0.50	20334.20	[0° 0° -10° 0° 0° 10° 0°] _s	2.52
Genetic Algorithm	P-100	Poliamide	0.40	3.9470	[0° -10° 0° 20° 0° 0° 0° 0° 10° 0° 0° -30° 10° 0° -10° -80°] _s	6.12
Simulated Annealing	*	*	*	*	*	*

Tabu Search	*	*	*	*	*	*
-------------	---	---	---	---	---	---

Table 7. P_k^i coefficients obtained in the best solution of VNS-based model

Lamina	P_k^i (VNS)	Lamina	P_k^i (VNS)
0°	0.64501	0°	0.64501
0°	0.64501	10°	0.91776
-10°	0.91776	0°	0.64501
0°	0.64501		

Table 8. Statistics corresponding to the series of tests

Algorithm	NL_{reduit}	N_i	\overline{NL}	σ_{NL}	F_{max}	\overline{F}
VNS-based model	8	300	8	0	$1.34 \cdot 10^8$	$1.34 \cdot 10^8$

Table 9. Characteristics of the best laminate obtained in a series of tests

Algorithm	Fibre	Matrix	VF	Fitness	Laminas	Thickness (mm)
VNS-based model	T-40	Polyester	0.60	$1.34 \cdot 10^8$	[0° 0° 0° 0°] _s	1.44

Table 10. P_k^i coefficients obtained in the best solution of VNS-based model

Lamina	P_k^i (VNS)	Lamina	P_k^i (VNS)
0°	0.99760	0°	0.99760
0°	0.99760	0°	0.99760

Table 11. Statistics corresponding to the series of tests

Algorithm	NL_{reduit}	N_i	\overline{NL}	σ_{NL}	F_{max}	\overline{F}
VNS-based model	20	5	24.5533	1.2672	52.0046	22.1605
Genetic Algorithm	26	13	40.24	11.0103	16.4138	2.5790
Simulated Annealing	28	2	51.9267	13.5403	4.8360	0.0708
Tabu Search	26	4	30.5467	3.0019	17.1439	0.2709

Table 12. Characteristics of the best laminate obtained in the series of tests

Algorithm	Fibre	Matrix	VF	Fitness	Laminas	Thickness (mm)
VNS-based model	P-100	Peek	0.50	52.0046	[-30° -30° -40° -40° 30° 40° -40° 40° 30° 40°] _s	3.60
Genetic Algorithm	P-100	Peek	0.40	16.4138	[10° -20° 0° 70° 20° 10° 10° -20° 10° -70° 70° -70° -30°] _s	4.68
Simulated Annealing	P-100	Peek	0.40	4.8360	[-40° 10° 70° -10° -10° 0° 0° 70° 50° 0° 0° 30° -30° -60°] _s	5.04
Tabu Search	P-100	Peek	0.40	17.1439	[-70° -30° 10° -30° 30° -40° 30° -40° -20° 40° 30° 50° 10°] _s	4.68

Table 13. P_k^i coefficients obtained in the best solution of VNS-based model

Lamina	P_k^i (VNS)	Lamina	P_k^i (VNS)
-30°	0.92702	40°	0.98502
-30°	0.92702	-40°	0.98502
-40°	0.98502	40°	0.98502
-40°	0.98502	30°	0.92702
30°	0.92702	40°	0.98502

Table 14. Statistics corresponding to the series of tests

Algorithm	NL_{reduit}	N_i	\overline{NL}	σ_{NL}	F_{max}	\overline{F}
VNS-based model	28	294	28.04	0.2805	3.4525	3.4017

Genetic Algorithm	36	2	61.58	13.4447	0.6419	0.0187
Simulated Annealing	44	1	71.48	16.8041	0.0056	$1.567 \cdot 10^{-4}$
Tabu Search	28	1	33.00	2.2037	3.1139	0.2749

Table 15. Characteristics of the best laminate obtained in the series of tests

Algorithm	Fibre	Matrix	VF	Fitness	Laminas (half a laminate)	Thickness (mm)
VNS-based model	P-100	Peek	0.50	3.4525	[40° -40° -40° 50° -50° 50° -40° -40° -50° 40° 40° 40° 50° 40°] _s	5.04
Genetic Algorithm	P-100	Peek	0.30	0.6419	[50° 30° -50° -50° 50° 50° -50° -40° 50° 50° 40° -40° -40° -50° 50° 50° 40° 40°] _s	6.48
Simulated Annealing	P-100	Poliamide	0.60	0.0056	[-40° -40° -50° 50° -40° 50° 40° 50° 40° 40° 40° -50° 50° 40° 50° 50° -50° 40° 40° -40° -40° -50°] _s	7.92
Tabu Search	P-100	Peek	0.50	3.1139	[40° 40° -40° 40° -40° -40° -40° 40° -40° -40° 40° 40° 40° 30° 50°] _s	5.04

Table 16. P_k^i coefficients obtained in the best solution of VNS-based model

Lamina	P_k^i (VNS)	Lamina	P_k^i (VNS)
40°	0.95535	-40°	0.91292
-40°	0.91292	-50°	0.96634
-40°	0.91292	40°	0.95535
50°	0.90230	40°	0.95535
-50°	0.96634	40°	0.95535
50°	0.90230	50°	0.90230
-40°	0.91292	40°	0.95535

Figure 1. Assessment of specific strength and stiffness between different composite materials and metals

Figure 2. Composition of a lamina and laminate construction

Figure 3. Basic scheme of the VNS algorithm

Figure 4. Example of the VNS model

Figure 5. Labeling criteria for the orientation of the laminas

Figure 6. Representation of the problem

Figure 7. Thin-walled ring under internal pressure

Figure 8. Histograms of the number of laminas and the fitness obtained by the VNS-based model

Figure 9. Thin-walled cylindrical tank subjected to interior pressure

Figure 10. Histograms of the number of laminas and the fitness obtained by the VNS-based model

Figure 11. Hollow driveshaft subjected to an external torque.

Figure 12. Histograms of the number of laminas and the fitness corresponding to a series of tests made with the VNS-based model.

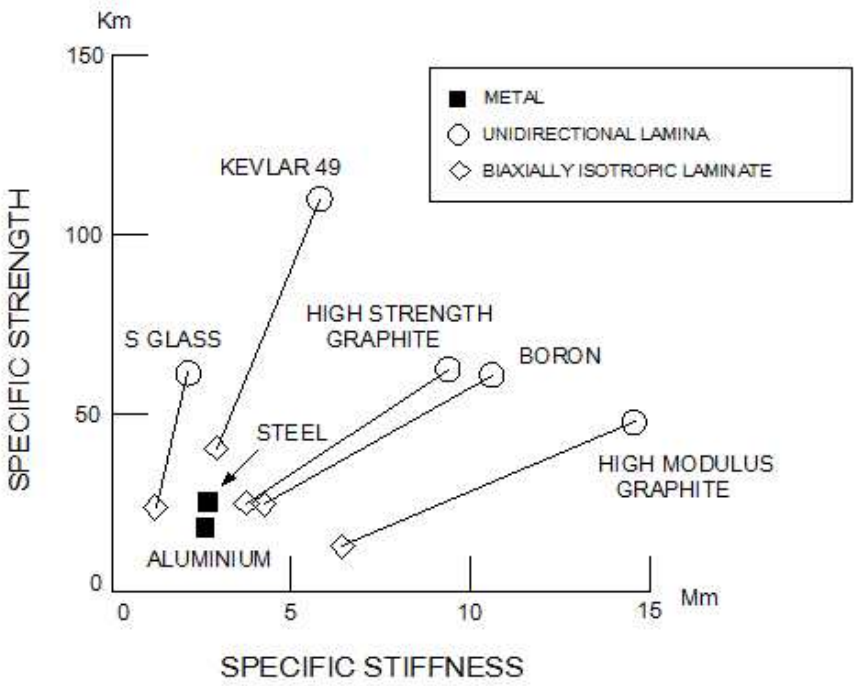


Figure 1. Assessment of specific strength and stiffness between different composite materials and metals
144x105mm (96 x 96 DPI)

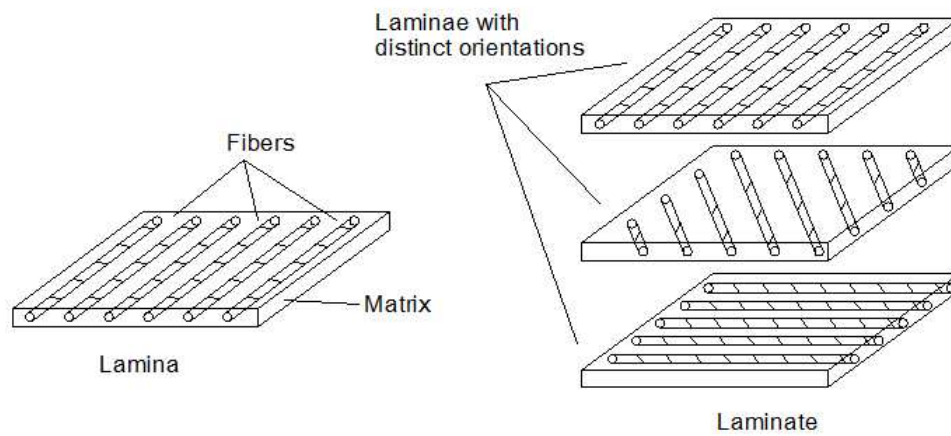


Figure 2. Composition of a lamina and laminate construction
188x91mm (96 x 96 DPI)

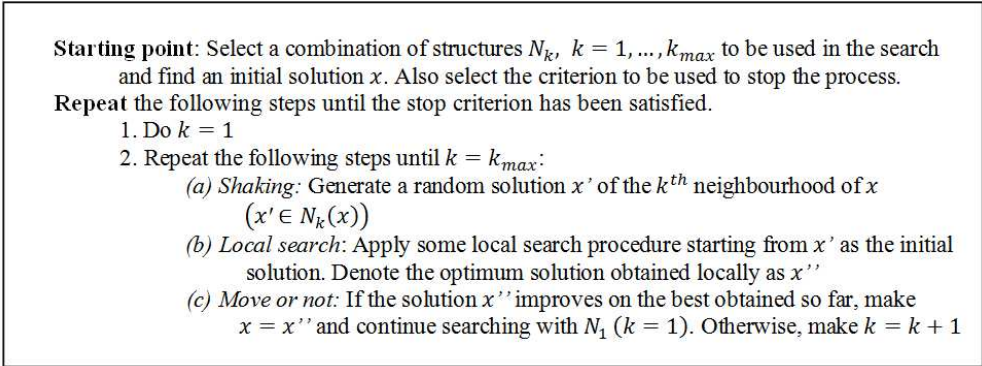


Figure 3. Basic scheme of the VNS algorithm
256x97mm (96 x 96 DPI)

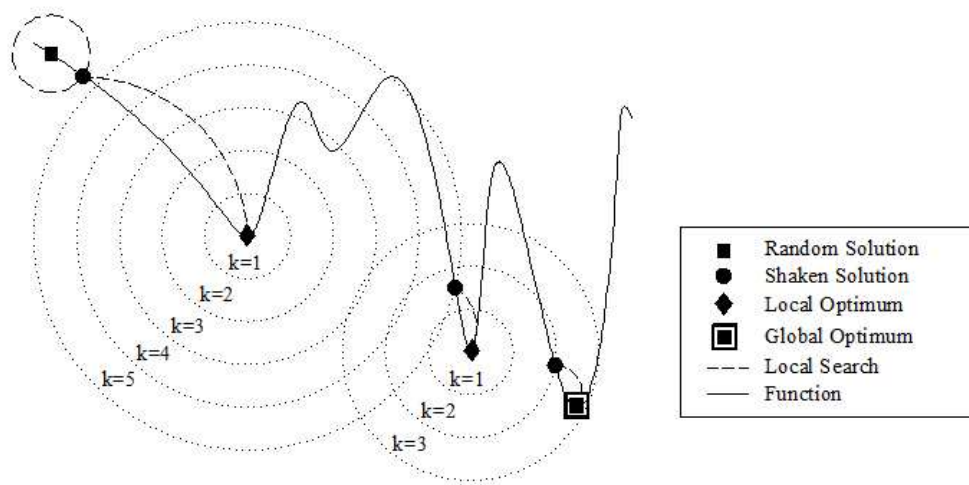


Figure 4. Example of the VNS model
184x91mm (96 x 96 DPI)

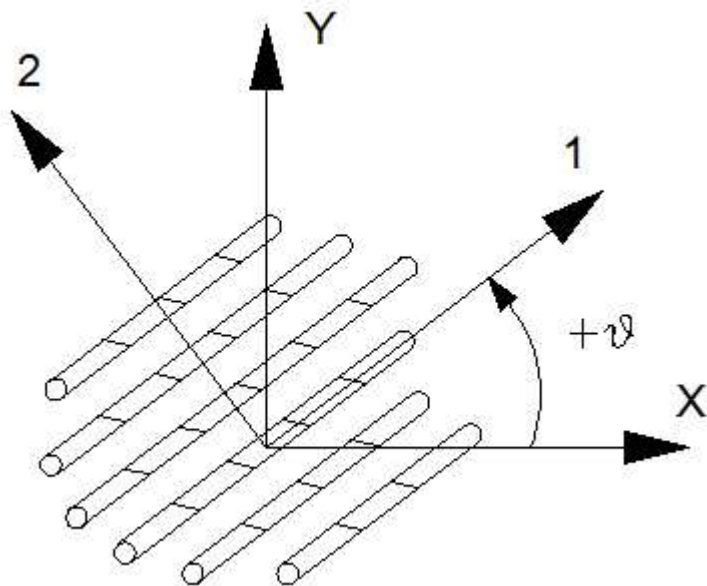


Figure 5. Labeling criteria for the orientation of the laminas
105x82mm (96 x 96 DPI)

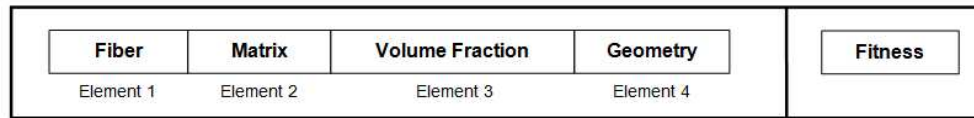


Figure 6. Representation of the problem
214x29mm (96 x 96 DPI)

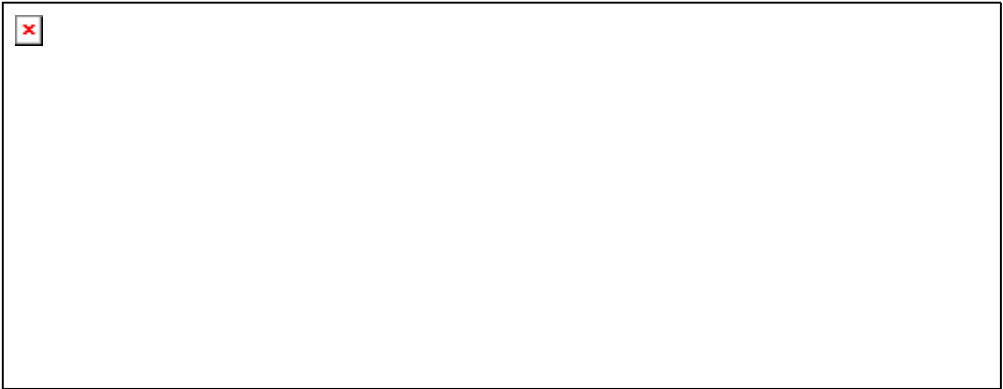


Figure 7. Thin-walled ring under internal pressure
279x108mm (96 x 96 DPI)

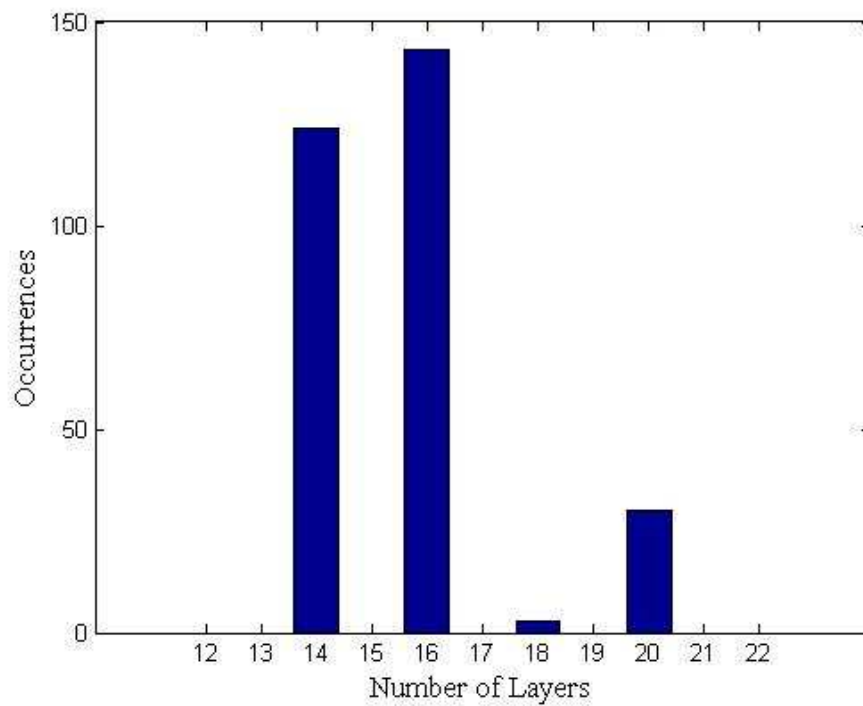


Figure 8a. Histograms of the number of laminas and the fitness obtained by the VNS-based model
148x111mm (96 x 96 DPI)

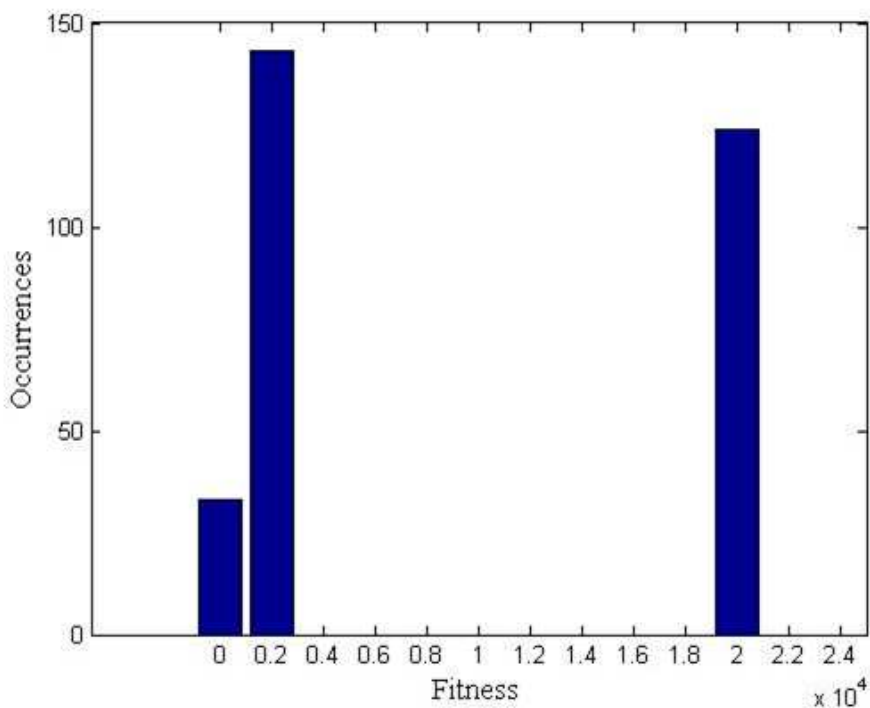


Figure 8b. Histograms of the number of laminas and the fitness obtained by the VNS-based model
148x111mm (96 x 96 DPI)

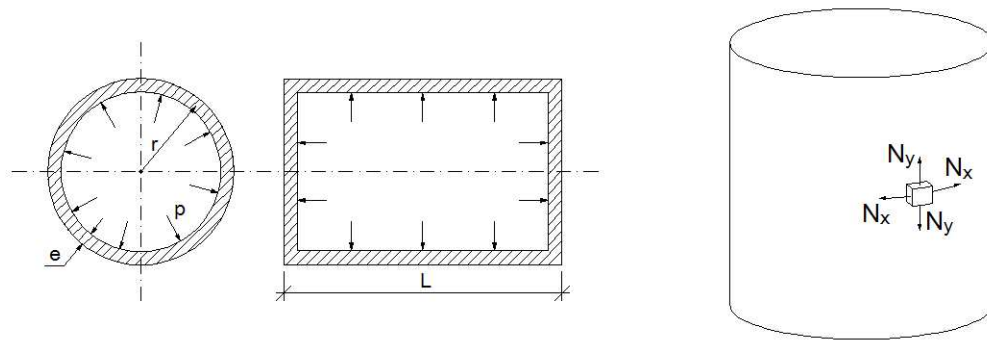


Figure 9. Thin-walled cylindrical tank subjected to interior pressure
275x98mm (96 x 96 DPI)

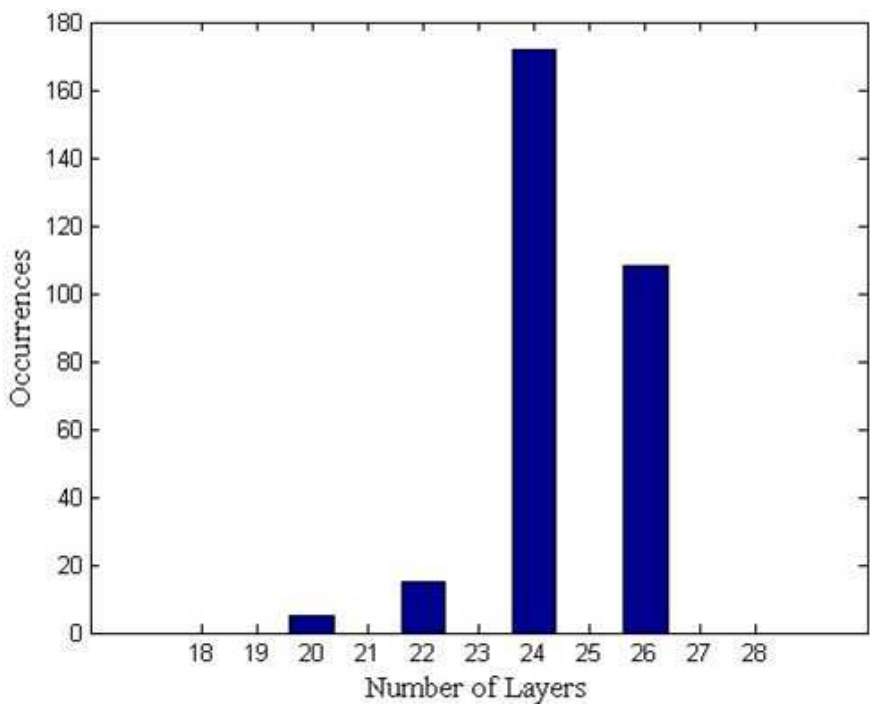


Figure 10a. Histograms of the number of laminas and the fitness obtained by the VNS-based model
148x110mm (96 x 96 DPI)

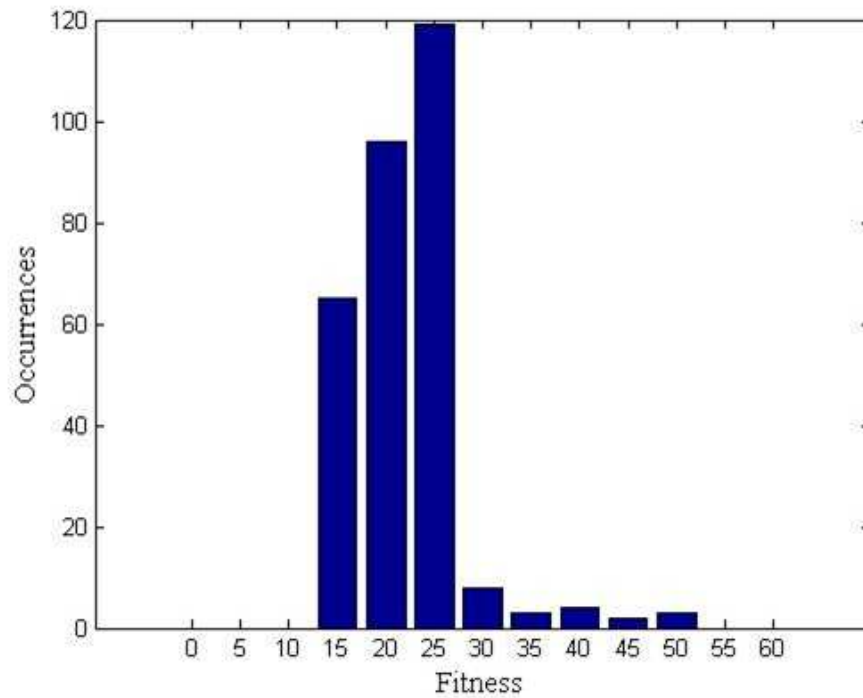


Figure 10b. Histograms of the number of laminas and the fitness obtained by the VNS-based model
148x110mm (96 x 96 DPI)

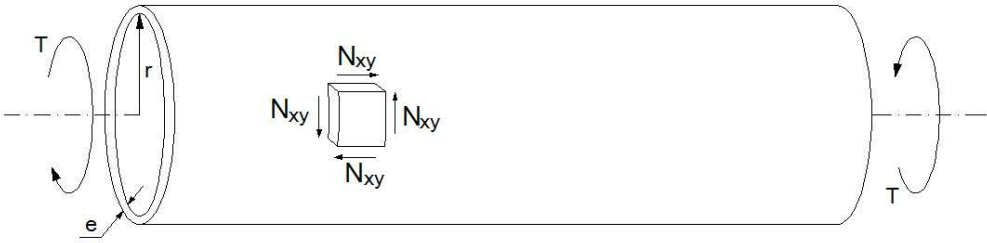


Figure 11. Hollow driveshaft subjected to an external torque
285x73mm (96 x 96 DPI)

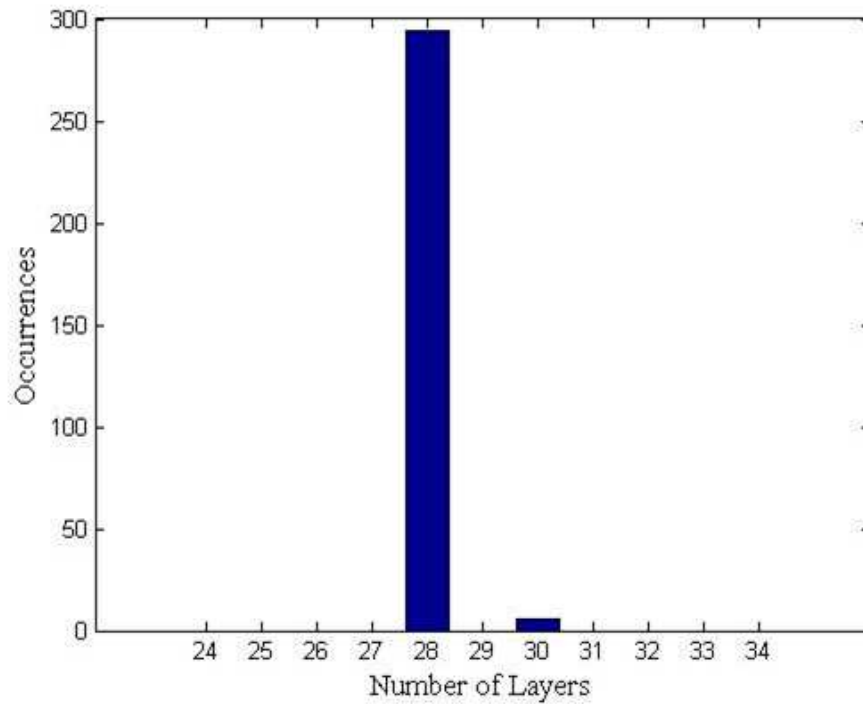


Figure 12a. Histograms of the number of laminas and the fitness corresponding to a series of tests made with the VNS-based model
148x111mm (96 x 96 DPI)

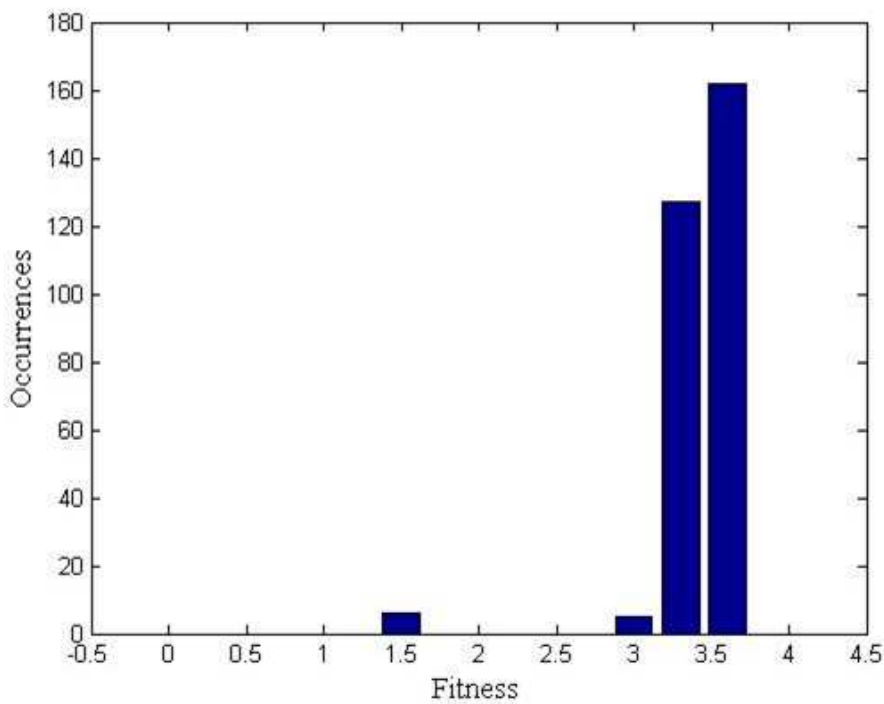


Figure 12b. Histograms of the number of laminas and the fitness corresponding to a series of tests made with the VNS-based model.
148x111mm (96 x 96 DPI)